International Journal of Engineering and Advanced Technology (IJEAT)
ISSN: 2249-8958 (Online), Volume-3 Issue-5, June 2014

Effects of Occupation Numbers on Charge Density Distributions, Elastic Form Factors, and Root-Mean Square Radii for Some Nuclei in 1s-1p Shell

Arkan R. Ridha, Wasan Z. Majeed, Ali D. Salloum

Abstract*— The effects of occupation numbers on the ground state charge density distributions, elastic form factors and root mean square (RMS) radii are investigated for 4He, 12C, and 16O nuclei in 1s-1p shell using single-particle radial wave functions of harmonic-oscillators (HO) potential. For such potential, two HO size parameters are used one for neutron ( ) and the other for proton ( ). For the calculated charge density distributions, the results showed good agreement with experimental data except the fail to produce the hump in the central region for 12C and 16O nuclei. For elastic charge form factors the results in general, showed excellent agreement to predict the positions of diffraction minima. The match of calculated charge form factor for 12C with experimental data was excellent at all q range, but for 4He and 16O it was obtained an underestimation at high q values. Finally, the calculated RMS charge radii in general, showed an overestimation comparing with those of experimental data, while those of matter showed excellent agreement with experiment.

Index Terms*— Stable Nuclei, Shell Model, Charge Density Distribution, Elastic Charge Form Factor, RMS Charge, Neutron, And Matter Radii.

I. INTRODUCTION

Nuclear size and density distribution are the basic quantities to describe the nuclear properties [1-3]. The charge densities can give us much detailed information on the internal structure of nuclei since they are directly related to the wave functions of protons, which are important keys for many calculations in nuclear physics. Electron–nucleus scattering is known to be one of the powerful tools for investigating nuclear charge density distributions. Charge density distributions for stable nuclei have been well studied with this method [4-6]. The comparison between calculated and measured electron scattering form factors has long been used as a successful test of nuclear models which have been adopted through the last fifty years. One of these models is the shell model [7] which is the most modern microscopic nuclear structure calculations for finite nuclei and has been very successful in describing the nuclear structure [8].

Manuscript published on 30 June 2014.
***** Correspondence Author (s)
Arkan R. Ridha, Department of Physics, University of Baghdad / College of Science / Baghdad, Iraq.
Wasan Z. Majeed, Department of Physics, University of Baghdad / College of Science / Baghdad, Iraq.
Ali D. Salloum, Department of Physics, University of Baghdad / College of Science for Women / Baghdad, Iraq.

Various theoretical methods are used for calculations of charge density distribution, among them the Hartree- Fock (HF) method with Skyrme effective interaction [9], the theory of finite Fermi system (TFTS) [10,11], the single particle potential method [12], phase- shift analysis method and the eikonal approximation [13]. The aim of the present work is to study the ground state charge density, RMS radii and elastic electron scattering form factors of ^{4}He, ^{12}C and ^{16}O nuclei. The charge density distribution of these nuclei is calculated by means of the harmonic-oscillator wave functions on the assumption that occupation numbers of the states in a real nucleus differ from the predications of the simple shell model.

II. THEORETICAL FORMULATIONS

The transition charge density one-body operator of rank J for point nucleons (with isospin $t_z = 1/2$) or neutrons ($t_z = -1/2$) can be written as [14]:

$$\hat{\rho}_J = \sum_{k=1}^{A} e(t_z) \frac{\delta(r - r_k)}{r^2} Y_{J,M_J}(\Omega_{r_k}), \quad (1)$$

where

$$e(t_z) = \frac{1 + 2t_z(k)}{2}.$$

In the above Eq. (1), $Y_{J,M_J}(\Omega_{r_k})$ and $\delta(\vec{r} - \vec{r}_k)$ are spherical harmonic and Dirac delta functions, respectively. The multipolarity J of the transition is restricted by the following angular momentum and parity selection rules:

$$\left| J_i \_ J_f \right| \le J \le J_i + J_f$$

and

$$\pi_i \pi_f = (-1)^J \quad \text{(for Coulomb transitions).}$$

The reduced matrix element of the transition charge density operator of Eq. (1), can be written as [14]:

$$\left\langle J_f \left\| \hat{\rho}_J(\vec{r}) \right\| J_i \right\rangle = \frac{1}{\sqrt{4\pi(2J_i + 1)}}$$

$$\cdot \sum_{ab} X_{a,b,t_z}^{J_f, J_i, J} \left\langle j_a \left\| Y_J \right\| j_b \right\rangle R_{n_a l_a}(r) R_{n_b l_b}(r), \quad (2)$$

where a and b stand for the single-particle states and are specified by:

Published By:
Blue Eyes Intelligence Engineering and Sciences Publication (BEIESP)

$|p\rangle = |n_p l_p\rangle |j_p m_p\rangle$, (the state p represents either a or b)

The states $|J_i\rangle$ and $|J_f\rangle$ are initial and final spin of the nuclei under study. In Eq. (2), $R_{n_p l_p}(r)$ is the radial part of the HO wave function, $\langle j_a \| Y_J \| j_b \rangle$ is the reduced matrix element of the spherical harmonic and $X^{J_f,J_i,J}_{a,b,t_z}$ is the proton ($t_z = 1/2$) or neutron ($t_z = -1/2$) one body density matrix element given by the second quantization as [14]:

$$X^{J_f,J_i,J}_{a,b,t_z} = \frac{\langle J_f \| [a^+_{a,t_z} \otimes \tilde{a}_{b,t_z}]^J \| J_i \rangle}{\sqrt{2J+1}} \quad (3)$$

The relation between these triply reduced $X^{J_f,J_i,J}_{a,b,t_z,\Delta T}$ and the proton or neutron $X^{J_f,J_i,J}_{a,b,t_z}$ of Eq. (2) is given by [15]:

$$X^{J_f,J_i,J}_{a,b,t_z} = (-1)^{T_f - T_z}\sqrt{2}\begin{pmatrix} T_f & 0 & T_i \\ -T_z & 0 & T_z \end{pmatrix}\frac{X^{J_f,J_i,J}_{a,b,t_z,\Delta T=0}}{2}$$

$$+ 2t_z(-1)^{T_f - T_z}\sqrt{6}\begin{pmatrix} T_f & 1 & T_i \\ -T_z & 0 & T_z \end{pmatrix}\frac{X^{J_f,J_i,J}_{a,b,t_z,\Delta T=1}}{2} \quad (4)$$

where the triply reduced $X^{J_f,J_i,J}_{a,b,t_z,\Delta T}$ elements are given in the second quantization as:

$$X^{\Gamma_f,\Gamma_i,J}_{\alpha,\beta,\Delta T} = \frac{\langle \Gamma_f \| [a^+_\alpha \otimes \tilde{a}_\beta]^{J,\Delta T} \| \Gamma_i \rangle}{\sqrt{2J+1}\sqrt{2\Delta T+1}} \quad (5)$$

Here, Greek symbols are utilized to indicate quantum numbers in coordinate space and isospace (i.e., $\Gamma_i \equiv J_i T_i$ and $\Gamma_f \equiv J_f T_f$).

The $X^{\Gamma_f,\Gamma_i,J}_{\alpha,\beta,\Delta T}$ elements contain all of the information about transitions of given multipolarities which are embedded in the model wave functions.

For the ground state density distribution, one has $J_i = J_f$, $J = 0$ and $a = b$ (i.e., $n_a = n_b$, $l_a = l_b$ and $j_a = j_b$). Therefore, the reduced matrix element of the spherical harmonic presented in Eq. (2) will give the following result [16]:

$$\langle j_a \| Y_0 \| j_a \rangle = (-1)^{2j_a+1}\sqrt{\frac{2j_a+1}{4\pi}} = \sqrt{\frac{2j_a+1}{4\pi}} \quad (6)$$

Substituting Eq. (6) into Eq. (2), one finds that:

$$\rho_{t_z}(r) = \frac{1}{4\pi\sqrt{(2J_i+1)}}\sum_\alpha \sqrt{2j_a+1}\, X^{J_i,J_i,0}_{a,a,t_z}\left|R_{n_a l_a}(r,b_{t_z})\right|^2 \quad (7)$$

where

$$\rho_{t_z}(r) = \langle J_i \| \hat{\rho}_J(\vec{r}) \| J_i \rangle .$$

In Eq. (7), b_{t_z} are the HO size parameters of protons ($t_z = 1/2$) and neutrons ($t_z = -1/2$).

It is worth mentioning that the final formula in Eq. (7) is normalized to the atomic number (Z) (point proton density) and neutron number (N) (point neutron density) as follows:

$$4\pi\int_0^\infty \rho_{p\,or\,n}(r) r^2 dr = Z \text{ or } N.$$

For pure configuration, $X^{J_i,J_i,0}_{a,a,t_z}$ can be written as [ ]:

$$X^{J_i,J_i,0}_{a,a,t_z} = \frac{\sqrt{2J_i+1}}{\sqrt{2j_a+1}} n_{a,t_z}, \quad (8)$$

where n_{a,t_z}, represents the number of neutrons ($t_z = 1/2$) or protons ($t_z = -1/2$) in the subshells.

Finally, Eq. (7) can be simplified with the aid of result in Eq. 8 to the form:

$$\rho_{t_z}(r) = \frac{1}{4\pi}\sum_a n_{a,t_z}\left|R_{n_a l_a}(r,b_{t_z})\right|^2 \quad (9)$$

The charge density distribution $\rho_{ch}(r)$ is obtained by folding the proton density ρ_{pr} into the distribution of the point protons of Eq. (9) as follows [17]:

$$\rho_{ch}(\vec{r}) = \int \rho_p(\vec{r})\rho_{pr}(\vec{r}-\vec{r}')d\vec{r}' \quad (10)$$

where ρ_{pr} takes the Gaussian form as [17]:

$$\rho_{pr}(r) = \frac{1}{\left(\sqrt{\pi}a_{pr}\right)^3} e^{\left(\frac{-r^2}{a^2_{pr}}\right)}, \quad (11)$$

and $a_{pr} = 0.65\ fm$. Such value of a_{pr} produces the experimental charge RMS radius of proton,

$$\langle r\rangle^{\frac{1}{2}}_{pr} = \left(\frac{3}{2}\right)^{1/2} a_{pr} \approx 0.8\ fm.$$

The charge RMS radii of can be directly deduced from their density distributions as follows [17]:

$$\langle r\rangle^{\frac{1}{2}}_{ch} = \sqrt{\frac{4\pi}{Z}\int_0^\infty \rho_{ch}(r) r^2 dr} \quad (12)$$

In plane wave Born approximation (PWBA) the elastic charge form factors are Fourier transform to their corresponding ground charge density distribution [17]:

$$F_{ch}(q) = \frac{4\pi}{qZ}\left[\int_0^\infty \rho_p(r)\sin(qr)rdr\right] f_{fc}(q) f_{cm}(q) \quad (13)$$

where $f_{fc}(q)$ and $f_{cm}(q)$ are free nucleon form factor and center of mass correction, respectively, given by [4]:

$$f_{fc}(q) = e^{\left(\frac{-0.43q^2}{4}\right)} \quad (14)$$

and

Published By:
Blue Eyes Intelligence Engineering and Sciences Publication (BEIESP)

$$f_{cm}(q) = e^{\left(\frac{b_p^2 q^2}{4A}\right)} \qquad (15)$$

where *A* in Eq. (15) represents the mass number of the nucleus under study.

It is worth mentioning that $F_{ch}(q)$ in Eq. (13) is normalized to unity in the limit $q \to 0$.

III. RESULTS AND DISCUSSION

In this work, the charge density distribution, RMS charge radii and elastic charge form factors are calculated in shell model using single-particle radial wave functions of harmonic-oscillators (HO) potential with two HO size parameters one for neutron (b_n) to reproduce the RMS matter radius and the second for proton (b_p) to reproduce RMS charge radius. The present calculations take two methods: the first uses the occupation numbers as predicted by simple shell model such calculations are denoted by SSM, the second method uses occupation numbers different from those predicted by SSM and controlled to reproduce the calculated charge density distribution, RMS charge radii and elastic charge form factors with experimental data, such method is denoted by MSM (modified shell model).

For ^{4}He nucleus, the HO size parameters for protons and neutrons are taken to be $b_n = 1.076\ fm$ and $b_p = 1.199\ fm$, respectively. The occupation numbers in SSM and MSM are tabulated in Tables [1] and [2], respectively. The calculated charge density distributions in SSM and MSM are displayed in Figure 1 by dashed and solid curves, respectively. It's clear from figure 1, that the result of the solid curve (MSM) is better than the calculation of dashed curve (SSM). This support the idea of the existence of strong mixing configuration between 1s and 1p shells according to $X_{a,a,t_z}^{J_i,J_i,0}$ suggested in Table [2]. The mixing coming from higher subshells leads to bad results comparing with experiment, therefore, the values of $X_{a,a,t_z}^{J_i,J_i,0}$ are restricted to these two suggested shells.

In figure 2, the calculated elastic charge form factors are displayed by dashed and solid curves calculated in SSM and MSM, respectively. The result of solid is better than the result of SSM in aspect of the position of first diffraction minimum which is well-predicted. The result of SSM completely fails to generate such position. Although the match with experimental data at high *q* values is bad, the result in general has good agreement with experiment.

In Table [3], the results of the calculated RMS charge, neutron, and matter radii are tabulated. The results of the calculated RMS charge and matter radii in SSM are in excellent agreement with experimental data on contrary to the results of the MSM which overestimate the result comparing with experimental data.

For ^{12}C nucleus, the values of the HO size parameters for protons and neutrons are taken to be $b_n = 1.5695\ fm$ and $b_p = 1.5846\ fm$, respectively. The occupation numbers in SSM and MSM are tabulated in Tables [4] and [5], respectively. In Figure 3, the calculated charge density distributions in SSM and MSM are displayed by dashed and solid curves, respectively. The result of the solid curve has a good agreement with experimental data, but there is a fail to generate the hump in the central region. This necessitates the importance of the existence of strong mixing configuration between 1s and 1d shells according to $X_{a,a,t_z}^{J_i,J_i,0}$ suggested in Table [5]. In figure 4, the results of the calculated elastic charge form factors are displayed by dashed and solid curves calculated in SSM and MSM, respectively. The result of solid curve has an excellent agreement with experimental data for all *q* values where the position of first diffraction minimum is also well-generated than the result of SSM which overestimates such position.

The calculated RMS charge, neutron, and matter radii are tabulated in Table [6]. The results of the calculated RMS charge and matter radii in SSM are again in excellent agreement with experimental data on contrary to the results of the MSM which overestimate the result comparing with experimental data.

For ^{16}O nucleus, the HO size parameters for protons and neutrons are taken to be $b_n = 1.466\ fm$ and $b_p = 1.70\ fm$, respectively. The occupation numbers are calculated in SSM and MSM and tabulated in Tables [7] and [8], respectively. The calculated charge density distributions in SSM and MSM are displayed in Figure 5 also by dashed and solid curves, respectively. It's obvious from such figure, that the result of solid curve is in fair agreement with experimental data. Suggesting the importance of being a strong mixing configuration between 1p and 1d shells according to $X_{a,a,t_z}^{J_i,J_i,0}$ presented in Table [8]. In figure 6, the calculated elastic charge form factors are displayed by dashed and solid curves calculated in SSM and MSM, respectively. The result of solid curve is more improved than the result SSM and the position of first diffraction minimum is well-predicted than the result of SSM which completely fail to generate such position. Although the match with experimental data at high *q* values is bad, the result in general has good agreement with experiment. The results of the calculated RMS charge, neutron, and matter radii are tabulated in Table [9]. The results of the calculated RMS charge and matter radii in MSM are also overestimated comparing with experiment, on contrary to the results of the SSM which slightly underestimate the result comparing with experimental data.

Published By:
Blue Eyes Intelligence Engineering
and Sciences Publication (BEIESP)

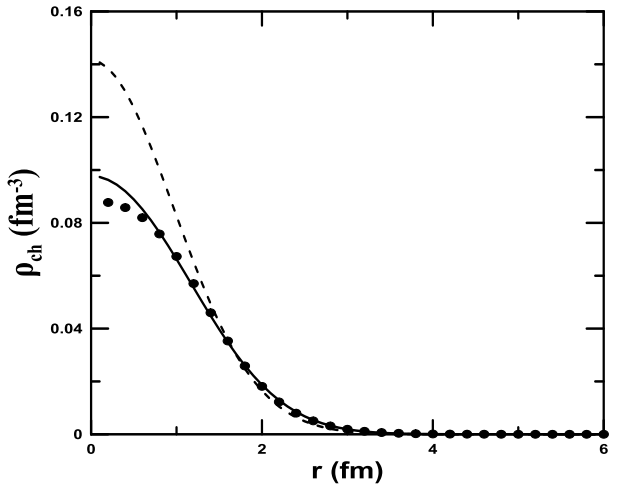

Fig.1. The calculated charge density distribution of ^{4}He nucleus. The dotted curve represents experimental data [18]. The dashed and solid curves are the calculated charge density using SSM and MSM, respectively.

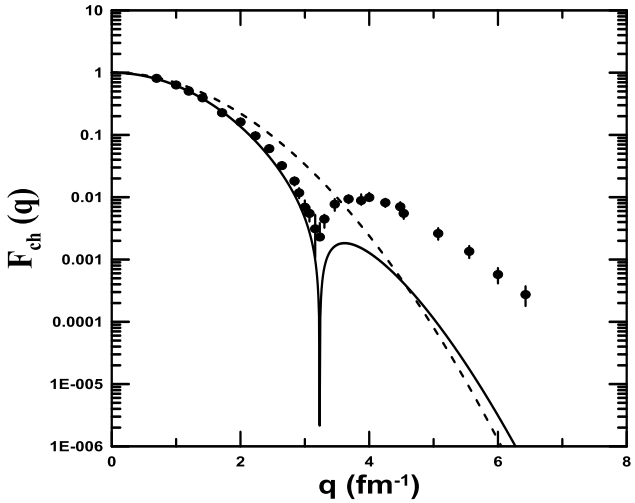

Fig.2. The elastic charge form factor of ^{4}He nucleus. The dotted curve represents experimental data [20, 21]. The dashed and solid curves are the calculated charge form factors calculated using SSM and MSM, respectively.

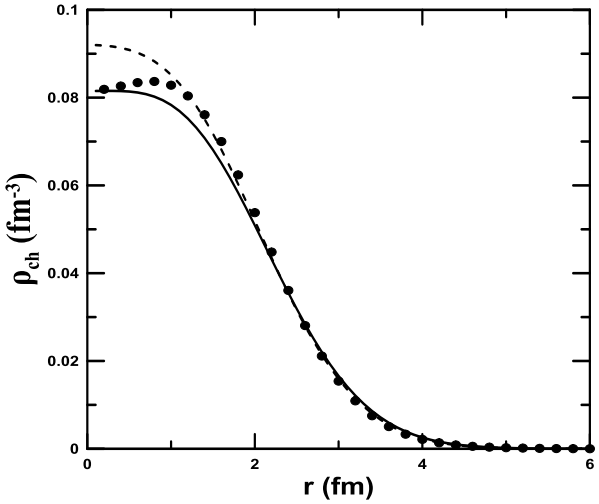

Fig.3. The calculated charge density distribution of ^{12}C nucleus. The dotted curve represents experimental data [18]. The dashed and solid curves are the calculated charge density using SSM and MSM, respectively.

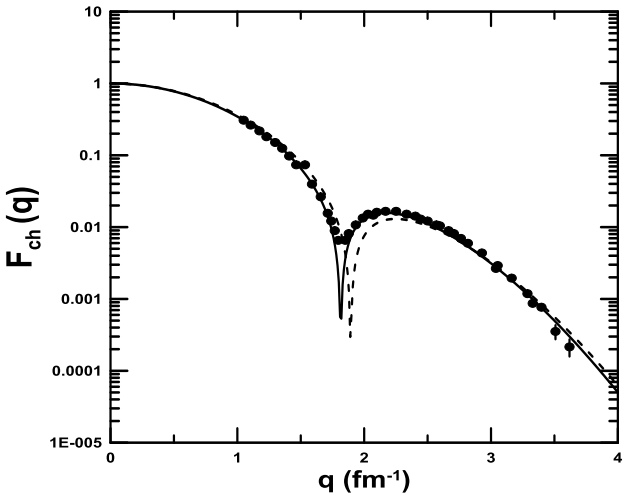

Fig.4. The elastic charge form factor of ^{12}C nucleus. The dotted curve represents experimental data [22]. The dashed and solid curves are the calculated charge form factors calculated using SSM and MSM, respectively.

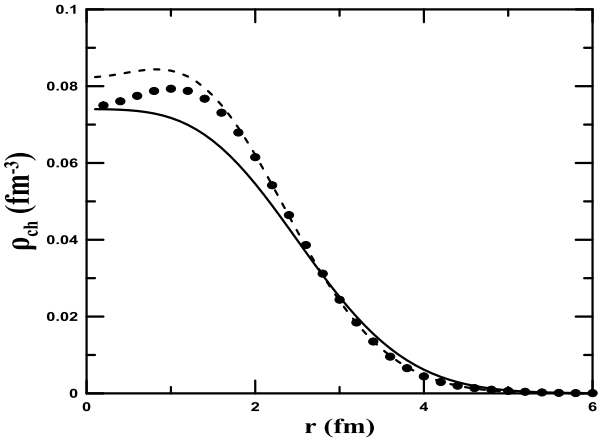

Fig.5. The calculated charge density distribution of ^{16}O nucleus. The dotted curve represents experimental data [18]. The dashed and solid curves are the calculated charge density using SSM and MSM, respectively.

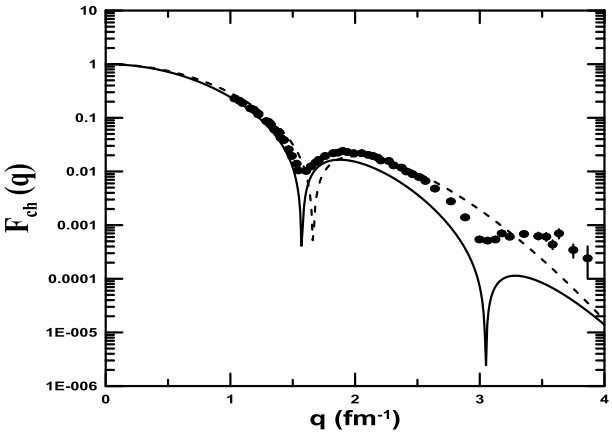

Fig.6. The elastic charge form factor of ^{16}O nucleus. The dotted curve represents experimental data [22]. The dashed and solid curves are the calculated charge form factors calculated using SSM and MSM, respectively.

Published By:
Blue Eyes Intelligence Engineering
and Sciences Publication (BEIESP)

IV. CONCLUSION

The ground state charge density distributions, elastic form factors and root- mean square (RMS) radii are studied for ^{4}He, ^{12}C, and ^{16}O nuclei in 1s-1p shell using shell occupation numbers different from those predicted by simple shell model. It was concluded that the mixing configuration between nuclear shells is important and needed to make the result in agreement with experimental data. The single-particle radial wave functions of harmonic-oscillators (HO) potential are used. Two HO size parameters are used one for neutron (b_n) and the other for proton (b_p) to reproduce the corresponding experimental data. The results of the calculated charge density distributions demonstrated good agreement with experimental data with the fail to reproduce the hump in the central region for ^{12}C and ^{16}O nuclei. In general, the calculations for elastic charge form factors showed excellent agreement to predict the positions of diffraction minima. An excellent match with experimental data for ^{12}C is obtained for the calculated charge form factor at all q range, but for ^{4}He and ^{16}O it was obtained an underestimation at high q values. Finally, the calculated RMS charge radii in general, showed an overestimation comparing with those of experimental data, while those of matter showed excellent agreement with experiment.

REFERENCES

[1] A. Bohr and B. R. Mottelson, *Nuclear Structure*. vol.1, Singapore: World Scientific, 1969, ch. 2.
[2] I. Tanihata, "Neutron halo nuclei," Journal of Physics G, Vol. 22, pp. 157-198. 1996.
[3] C. J. Batty, E. Friedman, H. J. Gils, and H. Rebel, "Experimental methods for studying nuclear density distributions," Advances in Nuclear Physics, Vol. 19, pp. 1-188, 1989.
[4] R. Hofstadter, "Electron Scattering and Nuclear Structure," Reviews of Modern Physics, Vol. 28, pp. 214-254, 1956.
[5] T.W. Donnelly and I. Sick, "Elastic magnetic electron scattering from nuclei, " Reviews of Modern Physics, Vol. 56, pp. 461-566, 1984.
[6] A. H. Wapstra, G. Audi, and R. Hoekstra, "Atomic masses from (mainly) experimental data, " Atomic Data and Nuclear Data Tables, Vol. 39, pp. 281-287, 1988.
[7] E. Caurier, G. Martinez-Pinedo, F. Nowacki, A. Poves, and A. P. Zuker, "The shell model as a unified view of nuclear structure, " Reviews of Modorn Physics, Vol. 77, pp. 427-488, 2005.
[8] W. C. Haxton and C.-L. Song, "Morphing the Shell Model into an Effective Theory," Physical Review Letters, Vol. 84, pp. 5484-5487, 2000.
[9] D. Vautherin and D. Brink, "Hartree-Fock Calculations with Skyrme's Interaction. I. Spherical Nuclei," Physical Review C, Vol. 5, pp. 626-.647, 1972.
[10] V. A. Khodel and E. E. Saperstein, "Finite Fermi systems theory and self-consistency relations," Physics Reports, Vol. 92, pp. 183-337, 1982.
[11] P. King and P. Schuck, *The nuclear many-body problem*. New York: Springer-Verlag, 1980, ch. 5.
[12] A. N. Antonon, P. E. Hodgson, and I. Zh. Petkov, *Nucleon momentum and density distributions in nuclei*. Oxford: Oxford university press,, 1988, ch. 4.
[13] Y. Chu, Z. Ren, T. Dong, and Z. Wang, "Theoretical study of nuclear charge densities with elastic electron scattering," Physical Review C, Vol. 79 (044313), pp. 1-7, 2009.
[14] B. A. Brown, R. Radhi, and B. H. Wildenthal, "Electric quadrupole and hexadecupole nuclear excitations from the perspectives of electron scattering and modern shell-model theory," Physics Reports. Vol. 101, pp. 313-358, 1983.
[15] R. A. Radhi, *Calculations of elastic and inelastic electron scattering in light nuclei with shell-model wave functions*. Ph.D.Thesis. Department of Physics, Michigan State University, USA. p.11, 1983.
[16] P. J. Brussard, and P. W. M. Glademans, *Shell model Applications in Nuclear Spectroscopy*. Amsterdam: North-Holland Publishing Company, 1977, appendix A.
[17] L. R. B. Elton, *Nuclear Sizes*. London: Oxford University Press, 1961, ch. 2.
[18] H. De Vries, C. W. De Jager, and C. De Vries, "Nuclear charge-density-distribution parameters from elastic electron scattering," Atomic Data and Nuclear Data Tables. Vol. 36, pp. 495-536, 1987.
[19] A. Ozawa, T. Suzuki, and I. Tanihata, "Nuclear size and related topics," Nuclear Physics A, Vol. 693, pp. 32-62. 2001
[20] R. Frosch, "Shell model analysis of elastic e^{-}-^{4}He scattering," Physics Letters B, Vol. 37, pp. 140-142, 1971.
[21] R. G. Arnold, B. T. Chertok, S. Rock, W. P. Schütz, Z. M. Szalata, D. Day, J. S. McCarthy, F. Martin, B. A. Mecking, I. Sick, and G. Tamas, "Elastic Electron Scattering from He3 and He4 at High Momentum Transfer," Physical Review Letters, Vol. 40, pp. 1429- 1432, 1978.
[22] I. Sick and J. S. McCarthy, "Elastic electron scattering from ^{12}C and ^{16}O," Nuclear Physics A, Vol. 150, pp. 631-654, 1970.

Published By:
Blue Eyes Intelligence Engineering
and Sciences Publication (BEIESP)

Table.1. The calculated $X_{a,a,t_z}^{J_i,J_i,0}$ for ^{4}He for neutrons and protons calculated in SSM

State 1	State 2	Number of protons ($n_{a,p}$)	Number of neutrons ($n_{a,n}$)	$X_{a,a,p}^{J_i,J_i,0}$	$X_{a,a,n}^{J_i,J_i,0}$
$1s_{1/2}$	$1s_{1/2}$	2.0	2.0	1.414214	2.000000

Table.2. The calculated $X_{a,a,t_z}^{J_i,J_i,0}$ for ^{4}He for neutrons and protons calculated in MSM

State 1	State 2	Number of protons ($n_{a,p}$)	Number of neutrons ($n_{a,n}$)	$X_{a,a,p}^{J_i,J_i,0}$	$X_{a,a,n}^{J_i,J_i,0}$
$1s_{1/2}$	$1s_{1/2}$	1.2	1.2	0.848528	0.848528
$1p_{3/2}$	$1p_{3/2}$	0.8	0.8	0.400000	0.400000

Table.3. The calculated RMS charge, neutron, and matter radii of ^{4}He

Technique	$\langle r\rangle_{ch}^{1/2}$	Exp. $\langle r\rangle_{ch}^{1/2}$ fm [18]	$\langle r\rangle_{n}^{1/2}$ fm	Exp. $\langle r\rangle_{n}^{1/2}$ fm	$\langle r\rangle_{m}^{1/2}$ fm	Exp. $\langle r\rangle_{m}^{1/2}$ fm [19]
SSM	1.670	1.671(14)	1.318		1.395	1.57(4)
MSM	1.834		1.483		1.570	

Table.4. The calculated $X_{a,a,t_z}^{J_i,J_i,0}$ for ^{12}C for neutrons and protons calculated in SSM

State 1	State 2	Number of protons ($n_{a,p}$)	Number of neutrons ($n_{a,n}$)	$X_{a,a,p}^{J_i,J_i,0}$	$X_{a,a,n}^{J_i,J_i,0}$
$1s_{1/2}$	$1s_{1/2}$	2.0	2.0	1.414214	1.414214
$1p_{3/2}$	$1p_{3/2}$	4.0	4.0	2.000000	2.000000

Table.5. The calculated $X_{a,a,t_z}^{J_i,J_i,0}$ for ^{12}C for neutrons and protons calculated in MSM

State 1	State 2	Number of protons ($n_{a,p}$)	Number of neutrons ($n_{a,n}$)	$X_{a,a,p}^{J_i,J_i,0}$	$X_{a,a,n}^{J_i,J_i,0}$
$1s_{1/2}$	$1s_{1/2}$	1.7	1.7	1.202082	1.202082
$1p_{3/2}$	$1p_{3/2}$	4.0	4.0	2.000000	2.000000
$1d_{5/2}$	$1d_{5/2}$	0.3	0.3	0.122474	0.122474

Table.6. The calculated RMS charge, neutron, and matter radii of ^{12}C

Technique	$\langle r\rangle_{ch}^{1/2}$	Exp. $\langle r\rangle_{ch}^{1/2}$ fm [18]	$\langle r\rangle_{n}^{1/2}$ fm	Exp. $\langle r\rangle_{n}^{1/2}$ fm	$\langle r\rangle_{m}^{1/2}$ fm	Exp. $\langle r\rangle_{m}^{1/2}$ fm [19]
SSM	2.464	2.464(12)	2.310		2.321	2.35(2)
MSM	2.514		2.363		2.374	

Published By:
Blue Eyes Intelligence Engineering and Sciences Publication (BEIESP)

Table.7. The calculated $X_{a,a,t_z}^{J_i,J_i,0}$ for ^{16}O for neutrons and protons calculated in SSM

State 1	State 2	Number of protons ($n_{a,p}$)	Number of neutrons ($n_{a,n}$)	$X_{a,a,p}^{J_i,J_i,0}$	$X_{a,a,n}^{J_i,J_i,0}$
$1s_{1/2}$	$1s_{1/2}$	2.0	2.0	1.414214	1.414214
$1p_{3/2}$	$1p_{3/2}$	4.0	4.0	2.000000	2.000000
$1p_{1/2}$	$1p_{1/2}$	2.0	2.0	1.414214	1.414214

Table.8. The calculated $X_{a,a,t_z}^{J_i,J_i,0}$ for ^{16}O for neutrons and protons calculated in MSM

State 1	State 2	Number of protons ($n_{a,p}$)	Number of neutrons ($n_{a,n}$)	$X_{a,a,p}^{J_i,J_i,0}$	$X_{a,a,n}^{J_i,J_i,0}$
$1s_{1/2}$	$1s_{1/2}$	2.0	2.0	1.414214	1.414214
$1p_{3/2}$	$1p_{3/2}$	1.5	1.5	0.750000	0.750000
$1p_{1/2}$	$1p_{1/2}$	2.0	2.0	1.414214	1.414214
$1d_{5/2}$	$1d_{5/2}$	2.5	2.5	1.020621	1.020621

Table.9. The calculated RMS charge, neutron, and matter radii of ^{16}O

Technique	$\langle r \rangle_{ch}^{1/2}$	Exp. $\langle r \rangle_{ch}^{1/2}$ fm [18]	$\langle r \rangle_{n}^{1/2}$ fm	Exp. $\langle r \rangle_{n}^{1/2}$ fm	$\langle r \rangle_{m}^{1/2}$ fm	Exp. $\langle r \rangle_{m}^{1/2}$ fm [19]
SSM	2.671	2.737 (8)	2.199		2.381	2.54 (2)
MSM	2.835		2.347		2.541	

Published By:
Blue Eyes Intelligence Engineering
and Sciences Publication (BEIESP)